

Tyrosine Nitration | Hot Paper |

Ni^{II}-ATCUN-Catalyzed Tyrosine Nitration in the Presence of Nitrite and Sulfite**Biplab K. Maiti, Luisa B. Maia, Isabel Moura, and José J. G. Moura*^[a]

Abstract: The nitration of tyrosine residues in proteins represents a specific footprint of the formation of reactive nitrogen species (RNS) in vivo. Here, the fusion product of orange protein (ATCUN-ORP) was used as an in vitro model system containing an amino terminal Cu(II)- and Ni(II)-binding motif (ATCUN) tag at the N-terminus and a native tyrosine residue in the metal-cofactor-binding region for the formation of 3-NO₂-Tyr (3-NT). It is shown that Ni^{II}-ATCUN unusually performs nitration of tyrosine at physiological pH in the presence of the NO₂⁻/SO₃²⁻/O₂ system, which is revealed by a characteristic absorbance band at 430 nm in basic medium and 350 nm in acidic medium (fingerprint of 3-NT). Kinetics studies showed that the formation of 3-NT depends on sulfite concentration over nitrite concentration suggesting key intermediate products, identified as oxysulfur radicals, which are detected by spin-trap EPR study by using 5,5-dimethyl-1-pyrroline-N-oxide (DMPO). This study describes a new route in the formation of 3-NT, which is proposed to be linked with the sulfur metabolism pathway associated with the progression of disease occurrence in vivo.

The formation of 3-nitrotyrosine (3-NO₂-Tyr=3-NT) in vivo is often related to several pathophysiological disorders, such as Alzheimer and Parkinson's diseases.^[1] The chemical origins of the formation of 3-NT in proteins have been proposed to occur through multiple pathways involving variable reactive nitrogen species (RNS); however, involvement of either peroxynitrite (ONOO⁻) or nitrogen dioxide (NO₂) is widely accepted for the formation of nitrated tyrosine through radical pathway promoted by transition metals (Fe, Cu, and Mn) or metalloproteins.^[2] The peroxynitrite-dependent and -independent pathways for protein tyrosine nitration are induced under biological conditions by superoxide dismutase (Cu-Zn-SOD^[3] and Mn-SOD^[4]) and heme-containing proteins, respectively.^[5] In addition,

in the presence of H₂O₂, metal ions (Fe^{II} and Cu^{II}) generate hydroxyl radicals (HO[•]) that oxidize NO₂⁻ to [•]NO₂ by Fenton reactions, leading to the production of 3-NT.^[6,7] So far, most of the studies have been focused on Fe-, Cu-, and Mn-based tyrosine nitration. However, Ni^{II} ions have not been considered for this reaction until now. Free Ni^{II} ions are physiologically redox inactive, and their toxicity in vivo has been related with activation by coordination with peptides and proteins with the histidine-containing motif (XXH) in the N-terminus, called ATCUN motif, which is found in several naturally occurring proteins.^[8,9] Ni^{II}-ATCUN promotes oxidative damage to DNA in the presence of H₂O₂^[9] or SO₃²⁻/O₂ due to the formation of hydroxyl or oxysulfur radicals (SO₃^{•-}, SO₄^{•-}),^[10] respectively. Therefore, sulfite exposure in humans can cause numerous diseases, such as asthma, chronic airway diseases, diarrhea, and neurological abnormalities.^[11,12] This exposure results from the inhalation of industrial SO₂,^[13] as well as from the intake of SO₃²⁻ (or HSO₃⁻) used as a preservative in food,^[11] alcoholic beverages, or drugs.^[14] Sulfite is also generated endogenously during the normal metabolism of sulfur-containing amino acids.^[15] In biology, sulfite is detoxified to sulfate by sulfite oxidase,^[16] to inhibit the formation of SO₃^{•-}, but cytotoxicity of (bi)sulfite occurs by the fatal loss of sulfite oxidase activity.^[17] The additive sulfite, in food, when mixed with salivary nitrite and, subsequently, with gastric juice in the stomach (pH ≈ 2–4), leads to nitric oxide (NO) production.^[18] The most relevant sources of nitrite are diet and nitric oxide catabolism.^[19] However, further chemistry using a NO₂⁻/SO₃²⁻/O₂ over a H₂O₂/NO₂⁻ or ONOO⁻ system as the nitrating source has not been explored for the formation of 3-NT under physiological conditions (pH ≈ 7.6).

To the best of our knowledge, this is the first report of 3-NT formation by a Ni^{II}-ATCUN in the presence of the NO₂⁻/SO₃²⁻/O₂ system. For this experiment, we used fusion orange protein (ATCUN-ORP) as an in vitro model complex containing ATCUN tag at the N-terminus (ASH) and native Tyr₇₅ located in cluster binding region of ATCUN-ORP (Figure 1).^[20,21] Recently, we have reported that cluster formation in ORP occur by protein–protein interaction in head-to-tail fashion, in which the N-terminus metal-binding ATCUN motif comes to the cluster-binding region, in which Tyr residues are affected through pseudocontact.^[20] Therefore, taking advantage of this model system, Ni^{II}-ATCUN-ORP was synthesized in the presence of NiCl₂ and apo-ATCUN-ORP at 1:1 ratio and characterized by UV/Vis absorption and ¹H NMR spectroscopic studies. The Ni^{II}-ATCUN-ORP can be oxidized by the H₂O₂ or SO₃²⁻/O₂ system and, subsequently, produce HO[•] or oxysulfur radicals, respectively, which are evaluated by EPR spectroscopy using 5,5-dimethyl-1-pyrroline N-

[a] Dr. B. K. Maiti, Dr. L. B. Maia, Prof. Dr. I. Moura, Prof. Dr. J. J. G. Moura LAQV, REQUIMTE, Departamento de Química, Faculdade de Ciências e Tecnologia Universidade Nova de Lisboa (FCT NOVA) Campus de Caparica, 2829-516 Caparica (Portugal) E-mail: jose.moura@fct.unl.pt

[**] ATCUN motif = amino terminal Cu(II)- and Ni(II)-binding motif.

Supporting information and the ORCID identification number(s) for the author(s) of this article can be found under: <https://doi.org/10.1002/chem.201806228>.

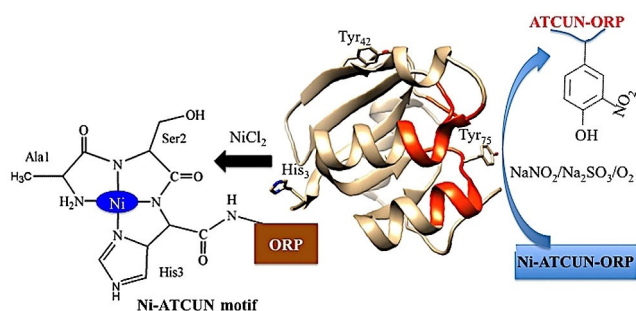


Figure 1. Crystal structure of apo-ATCUN-ORP showing only His₃ (ATCUN tag = ASH₃) and native Tyr_{75/42} residues. Highlighted metal-binding region (reddish-orange) containing conserved residues D₂₁PRFGRA₂₇, H₅₃GAGIN₅₈, and L₇₂TGYVGPKAF₈₁. Structures of apo-ATCUN-ORP (*D. gigas*) are deduced from PDB file 2wfb, see Ref. [21]. Ni-ATCUN catalyzed Tyr to 3-NO₂-Tyr in the presence of Na₂NO₂/Na₂SO₃/O₂.

oxide (DMPO) as the spin trap. The oxysulfur radicals may be scavenged by NO₂⁻ and Tyr to yield 3-NT, which is characterized by UV/Vis absorption spectra. The kinetic studies show that the formation of 3-NT depends on SO₃²⁻ concentration over NO₂⁻ concentration. Interesting, Ni-ATCUN is unable to produce tyrosine nitration in the presence of the H₂O₂/NO₂⁻ system.

The apo-ATCUN-ORP (300 μM) was incubated with NiCl₂ (300 μM) in 1:1 ratio to yield Ni^{II}-ATCUN-ORP derivative, which shows an absorbance peak at 420 nm ($\epsilon \approx 172 \text{ M}^{-1} \text{ cm}^{-1}$) (Figure S1, Supporting Information) and similar to other Ni^{II}-ATCUN site.^[6] The ¹H NMR spectrum of Ni^{II}-ATCUN-ORP (upon addition of 80% NiCl₂ to apo-ATCUN-ORP) shows that intensity and position of the His_{3/53} peaks (a = 7.643, b = 7.625, d = 6.903, and e = 6.890 ppm) are decreased and shifted (Figure 2). Furthermore, three new peaks (i = 7.672 ppm, ii = 7.381 ppm, and iii = 6.828 ppm) appeared. The two highly affected His₃ protons, a and e, are shifted to i and ii, respectively, supporting the notion of a direct contact between this His₃ and Ni^{II}.^[22] Peak iii at 6.85 ppm (doublet) may correspond to the H_δ/H_ε of Tyr₇₅, according to previous NMR data,^[23] this means that the Ni^{II}-ATCUN motif in Ni^{II}-ATCUN-ORP interacts with the aromatic group of the Tyr residue. In the aliphatic region, only the alanine site resonances at 1.310 and 1.298 ppm are highly affected (not shown) in a similar manner to Cu-ATCUN-ORP,^[20] but the Met signals at 1.987 and 1.890 ppm are not affected.

Ni^{II}-ATCUN-ORP is highly air stable. It can be oxidized by H₂O₂ to yield a new band at 372 nm with a shoulder at 420 nm (Figure S3, Supporting Information). The band at 372 nm may either be ascribed to Ni^{III}-ATCUN-ORP^[24] or disproportionation of Ni^{III} to form a Ni^{IV}=O intermediate, producing a hydroxyl radical that abstracts hydrogen atoms from amino acids in its vicinity in a common oxidative pathway.^[25] The literature data support the proposal that Ni^{II}-ATCUN-ORP undergoes the same pathway in the presence of H₂O₂ to generate HO[•] (see EPR experiment discussion) and activates the redox-active amino acid residue in the vicinity (see discussion on NMR analysis). The kinetics results indicate that the intensity of absorbance band at 372 nm increases at higher concentrations of H₂O₂, resulting in more production of HO[•] (Figure S3, Supporting Information).

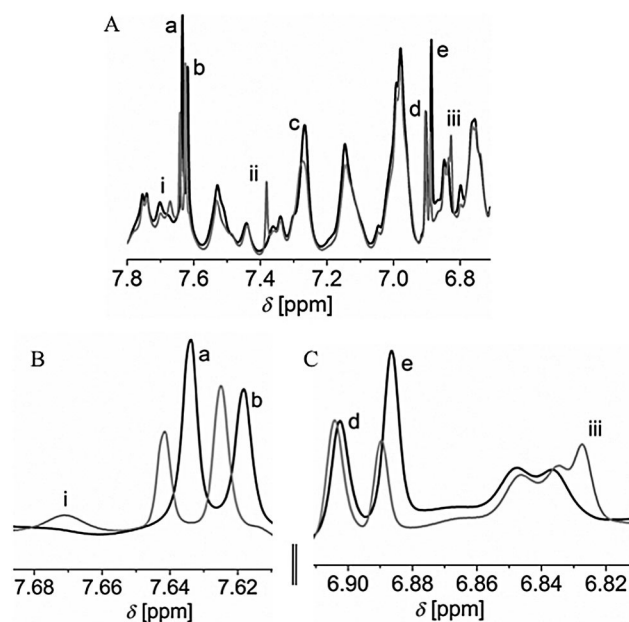


Figure 2. A) Aromatic region (7.8–6.7 ppm) of the ¹H NMR spectrum (600 MHz) of apo-ATCUN-ORP (1.5 mM; black), in 50 mM Tris-HCl at pH 7.6/ D₂O (80:20) with 80% NiCl₂ (grey). The highly affected peaks are indicated by a, b, c, d, e, i, ii, and iii. Magnification of B) i, a, and b peaks, and C) d, e, and iii peaks.

¹H NMR spectra of oxidized Ni^{II}-ATCUN-ORP were also obtained upon addition of 2 mM H₂O₂ to a solution (Figure 3). The intensity of peaks i, ii, and iii decreases and their positions shift to 7.701 (i), 7.394 (ii), and 6.873–6.867 ppm (iii), respectively. Peak iii (doublet) may correspond to the H_δ/H_ε protons of oxidized tyrosine. Peaks i (singlet) and ii (singlet) are shifted and assigned to His₃ proton resonances (H_ε and H_δ) as a result of the oxidation at Ni^{II}-ATCUN environment or influenced by oxidized Tyr. The physical meaning of these spectral findings may be interpreted due to the fact that the Ni^{II}-ATCUN site produces a HO[•] in the presence of H₂O₂, which can oxidize the tyrosine residue.^[26] In the aliphatic region, Met is also oxidized resulting in a decreased of the intensity of the peak at 1.987 ppm (f), and in the appearance of three new peaks at 2.623 (v), 2.581 (v_a), and at 2.555 ppm (v_b). The v_a and v_b signals are assigned to the methyl protons of -S(O)-CH₃ of the R and S forms.^[27] Peak v is also attributed to the -S(O)-CH₃ methyl group, but could only be seen in oxidized apo-ATCUN-ORP (Figure S2 in the Supporting Information; not in oxidized Ni-ATCUN-ORP).^[20]

Besides the use of H₂O₂, in this study, Ni^{II}-ATCUN-ORP was oxidized in the presence of SO₃²⁻/O₂ and the UV/Vis absorption spectrum shows a charge-transfer band at approximately 372 nm (Figure S4, Supporting Information) that is similar to the H₂O₂ oxidation method and also other reported Ni^{III}-peptide with sulfite oxidation.^[28] The sulfite autooxidation by Ni^{II}-ATCUN-ORP produce reactive oxysulfur radicals. The kinetic measurements were performed at variable SO₃²⁻ concentrations and the optical density values at 372 nm are reported as a function of time in Figure 4. The absorbance versus time traces clearly showed that initially (within approximately 2 min)

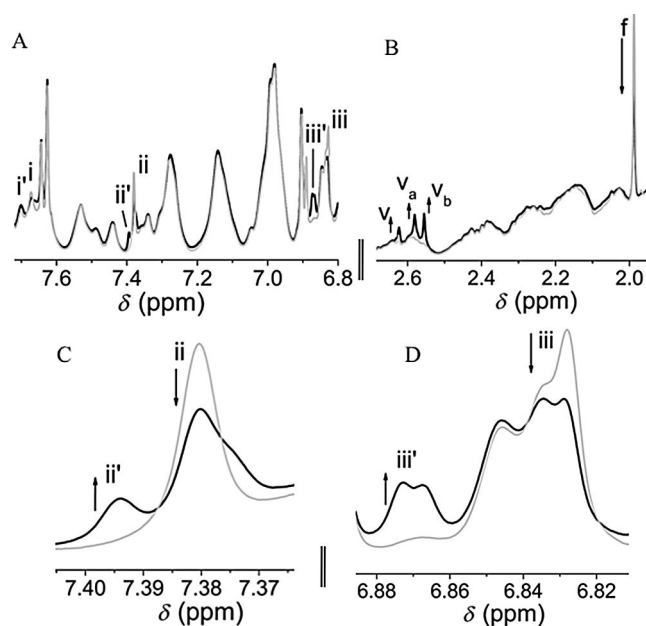


Figure 3. A) Aromatic region (7.7–6.7 ppm) of the ^1H NMR (600 MHz) spectrum of apo-ATCUN-ORP (1.5 mM) with 80% NiCl_2 (grey), and with 2 mM H_2O_2 after 1 h (dotted black) and 2 h (black) in 50 mM Tris-HCl at pH 7.6/ D_2O (80:20); i (i'), ii (ii'), and iii (iii') indicate highly affected peaks. B) The highly affected peaks in the aliphatic region (2.7–1.95 ppm) are indicated by v, v_a , v_b , and f. Magnification of C) ii and ii' peaks, and of D) iii and iii' peaks. Arrows indicate the direction of peak intensity variation.

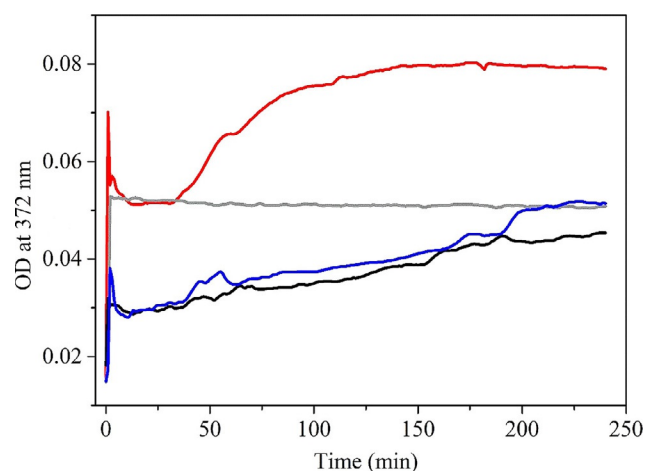


Figure 4. Kinetic measurements. $\text{OD}_{372\text{nm}}$ vs. time for Ni^{II} -ATCUN-ORP (300 μM) with 200 μM (grey), 500 μM (red), 1 mM (blue), and 2 mM (black) Na_2SO_3 in 50 mM Tris-HCl, pH 7.6 at RT.

the intensity increased at 372 nm and decreased after a certain time, depending on the concentration of Na_2SO_3 , and then increased again. The spectra are wave-like, indicating that Ni^{II} and Ni^{III} compete with O_2 and SO_3^{2-} . In an air-saturated solution and in the presence of 0.5 mM SO_3^{2-} , the intensity is maximum and, in the presence of more than 1 mM SO_3^{2-} , the formation of oxidized species is low. It means that initially Ni^{III} forms rapidly, but it does not stabilize, resulting in the decomposition to Ni^{II} or reduction by excess Na_2SO_3 (high concentration decreased). Considering that Ni^{II} -ATCUN-ORP is highly air

stable, Ni^{II} is oxidized by O_2 a process initiated by trace levels of SO_3^{2-} .^[29]

Our aim was to synthesize 3-NT with Ni^{II} -ATCUN-ORP in the presence of H_2O_2 and NaNO_2 , and monitor the reaction by spectroscopy. In this assay, 300 μM of Ni^{II} -ATCUN-ORP was incubated with 1 mM NaNO_2 and 1–5 mM H_2O_2 solution mixture, in 50 mM Tris-HCl, pH 7.6 at RT under air over 6–12 h. In this assay, no 3-NT was obtained, as revealed by monitoring the absorbance at 430 nm by UV/Vis spectroscopy (not shown). In the presence of H_2O_2 , Ni-ATCUN-ORP can produce hydroxyl radicals (see EPR experiments); thus, nitration of tyrosine should be obtained from this $\text{H}_2\text{O}_2/\text{NO}_2^-$ system by Fenton reaction pathway, like the Cu and Fe systems.^[6,7] Nevertheless, our in vitro model system is unable to produce 3-NT with the $\text{H}_2\text{O}_2/\text{NO}_2^-$ system. It is suggested that the methionine residue is very close to Ni^{II} -ATCUN in ATCUN-ORP and it can be easily oxidized by the hydroxyl radical to produce methionine sulfoxide,^[27] which was detected by NMR spectroscopy (see Figure 3, NMR section). In addition to the oxidation of Met residue, we also observed that HO^\bullet may oxidize other redox-active amino acid residues in the vicinity, such as Tyr residue in ATCUN-ORP to a limited amount of Tyr $^\bullet$, but without formation of NO_2^\bullet from NO_2^- . It is known that the neighboring methionine residue, in proteins and peptides, inhibits tyrosine nitration because methionine can be easily oxidized by reactive nitrogen and oxygen species.^[30]

We further investigated the formation 3-NT from the $\text{NaNO}_2/\text{SO}_3^{2-}/\text{O}_2$ system by using the Ni^{II} -ATCUN-ORP model. In this assay, 300 μM of Ni^{II} -ATCUN-ORP was incubated in a NaNO_2 (1 mM) and Na_2SO_3 (1 mM) solution in 50 mM Tris-HCl, pH 7.6, at RT under air over 6 h. Figure 5 shows an absorbance band at 430 nm, which is attributed to 3-NT; under acidic conditions, the UV/Vis absorption spectrum is shifted to 350 nm, whereas under basic conditions, it is shifted to 430 nm and vice versa, which is a fingerprint of 3-NT.^[31] The kinetics measurements of 3-NT formation were performed at various SO_3^{2-} concentrations with fixed amount of NO_2^- , for which typical absorbance (at 430 nm) versus time traces are reported in Figure 5 (inset). In this assay, 1–5 mM of Na_2SO_3 and 1 mM of nitrite were added to 300 μM of Ni-ATCUN-ORP in 50 mM Tris-HCl, pH 7.6 at RT under air and nitration was monitored in the UV/Vis region. The Figure 5 (Inset) clearly shows that the intensity increases at 430 nm with high concentration of Na_2SO_3 with time. To verify the reactivity of Ni^{II} ion and O_2 , kinetic measurements were carried out on two sets of samples at 430 nm under the same reaction conditions: one sample without NiCl_2 , and the other without O_2 (anoxic conditions; Figure 5, inset). In both cases, no increase of the band at 430 nm was observed, meaning that 3-NT did not form. To further examine the role of NO_2^- in the formation of 3-NT, we compared the nitration reaction by using different concentrations (1–5 mM) of NO_2^- and a fixed amount (1 mM) of SO_3^{2-} ; tyrosine nitration was monitored by UV/Vis absorption spectroscopy (Figure S5, Supporting Information). In this assay, the intensity at 430 nm of the formation of 3-NT is the same in all cases. This means that 3-NT formation depends on SO_3^{2-} concentration rather than on NO_2^- concentration.

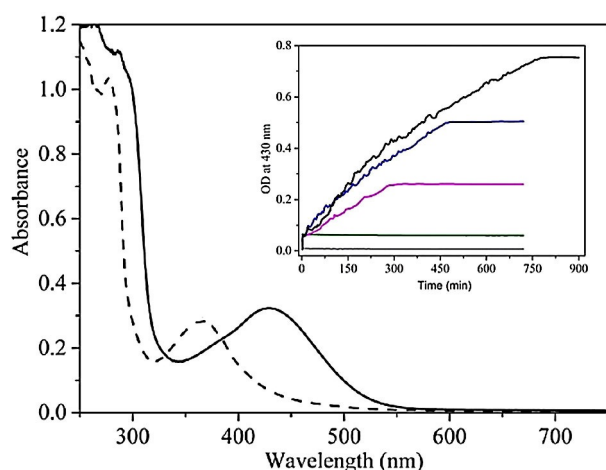


Figure 5. UV/Vis absorption spectra of Ni^{II}-ATCUN-ORP (300 μ M) with (1 mM Na₂SO₃ + 1 mM NaNO₂) in 50 mM Tris-HCl pH 7.6 after 6 h and desalting by PD-10 (black line), addition of 5–8 μ L 1 M of HCl, at pH about 5 (dotted line) at RT. Inset: Formation of 3-NT in the reaction of Ni^{II}-ATCUN-ORP (300 μ M) with 1 mM Na₂NO₂ and variable Na₂SO₃ concentration (1–5 mM) followed by measuring the absorbance at 430 nm (kinetics OD_{430nm} vs. time); 1 mM (purple), 2 mM (blue) and 5 mM (black) of Na₂SO₃ over 12 h under air at RT in 50 mM Tris-HCl, pH 7.6. The kinetic study of apo-ATCUN-ORP with 1 mM Na₂NO₂ and 2 mM Na₂SO₃ (grey line) over 12 h under air at RT in 50 mM Tris-HCl, pH 7.6. The kinetic study of Ni^{II}-ATCUN-ORP with 1 mM Na₂NO₂ and 2 mM Na₂SO₃ (green line) over 12 h under argon at RT in 50 mM Tris-HCl, pH 7.6.

The Ni^{II}-ATCUN-ORP is EPR silent. When 1.5 mM Ni^{II}-ATCUN-ORP (Ni:ORP 1:1) was incubated with 5 mM H₂O₂ for 3 min, 1, 2 and 4 h, no Ni^{III} (or Ni^I) signal was observed. Yet, a very weak and sharp (Δ_{pp} = 1.0 mT) signal at $g \approx 2$ (Figure S6, Supporting Information) emerged after incubation for 2 h (stable until 4 h), consistent with an organic radical (proposed to be a tyrosine radical; see details explanation in the Supporting Information) present in a very small concentration.^[26,32] In this assay, formation of other radical species (HO[•]) was identified by using spin-trap DMPO. After 3 min incubation, the signal characteristic of the HO[•]-DMPO adduct emerged [$a(H)$ = 1.47 mT and $a(N)$ = 1.69 mT; Figure 6A].^[33] Incubation with 5 mM SO₃²⁻ (with or without 1 mM NO₂⁻) to 1.5 mM Ni^{II}-ATCUN-ORP, produces neither amino acid radical species in ATCUN-ORP nor Ni^{III} (or Ni^I) up to 8 h of incubation. However, the formation of the SO₃⁻ was clearly identified by using spin-trap DMPO [$a(H)$ = 1.62 mT and $a(N)$ = 1.45 mT; Figure 6B].^[34] The intensity of the SO₃⁻-DMPO adduct signal, in the presence of nitrite (dark red spectra), increases until 30 min of incubation, after which it starts to slowly decrease. Alternatively, in the absence of nitrite (orange spectra), the SO⁻ signal intensity reaches its maximum at 6 h and afterwards decreases. This means that the formation of oxysulfur radical is scavenged by nitrite to yield transient species (NO₂⁻) and that the intensity decrease is relatively fast when the complete system is considered.

To understand the role of Ni^{II} in the formation of oxysulfur radicals, we carried out the reaction in deionized water with NiCl₂ and the NO₂⁻/SO₃²⁻/O₂ system, resulting in no formation of oxysulfur radical (no EPR signal). In the presence of 50 mM Tris-HCl buffer, pH 7.6, the Ni^{II}(N_{Tris})_x complex is generated,

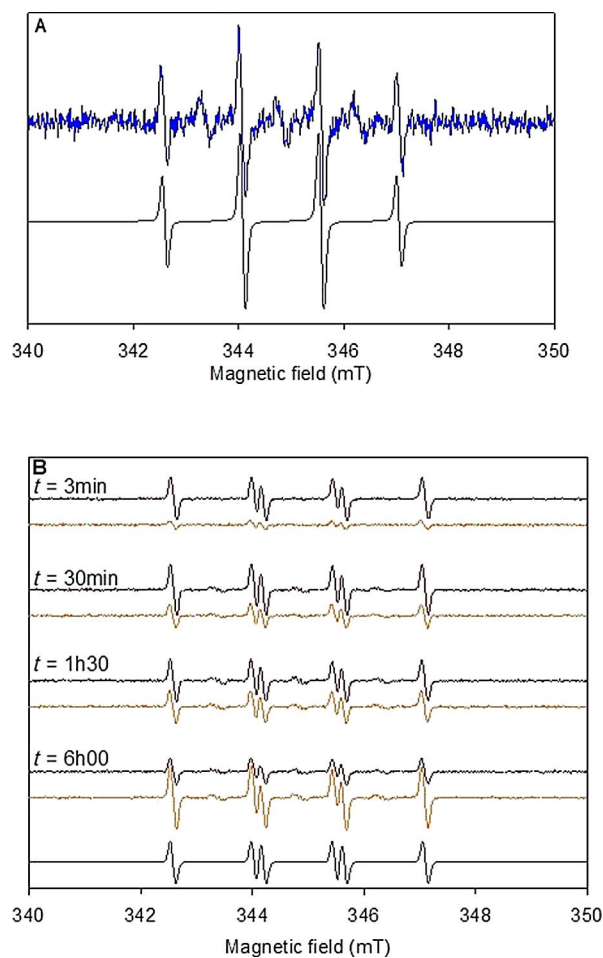


Figure 6. Spin-trap EPR study. A) 5 mM Ni^{II}-ATCUN-ORP (Ni/ORP 1:1) was incubated with 5 mM H₂O₂ for 3 min in the presence of DMPO, and the EPR spectrum (blue spectrum) was acquired at 293 K. The HO[•]-DMPO adduct signal was simulated with $a(H)$ = 1.47 mT and $a(N)$ = 1.69 mT (grey spectrum). Experimental spectra were acquired as described in the section “Materials and Methods” in the Supporting Information. Radical species formation in Ni^{II}-ATCUN-ORP reacted with the NO₂⁻/SO₃²⁻/O₂ system. B) 1.5 mM Ni^{II}-ATCUN-ORP (Ni:ORP 1:1) was incubated, in the presence of DMPO, with 5 mM SO₃²⁻, in the absence (orange spectra) or presence (dark-red spectra) of 1 mM NO₂⁻, for the time period indicated, and the EPR spectra were acquired at 293 K, as described in the “Materials and Methods” section in the Supporting Information. The SO₃⁻-DMPO adduct signal was simulated with $a(H)$ = 1.62 mT and $a(N)$ = 1.45 mT (grey line).

which produces a small amount of oxysulfur radical (not shown). Therefore, free Ni^{II} is not toxic, but in the presence of N-donor systems (like peptide, protein and small ligands) Ni^{II} shows toxicity.

Based on the spectroscopic results and the conclusions drawn from the kinetic experiments, the following mechanism is proposed for (NO₂⁻/SO₃²⁻/O₂) + Ni^{II}-ATCUN mediated tyrosine nitration in ATCUN-ORP (Figure 7). In the first step, Ni^{II}-ATCUN-ORP is oxidized to Ni^{III}-ATCUN-ORP by O₂ and initiated by traces of SO₃²⁻. After formation of the unstable Ni^{III}-ATCUN-ORP, which oxidizes SO₃²⁻/O₂ to generate SO₃⁻. Radical anion SO₃⁻ immediately reacts with O₂ to yield another oxysulfur radical, SO₅⁻, which is highly reactive and dimerizes to yield SO₄⁻ and O₂.^[10,34] Many types of oxysulfur radicals form in this

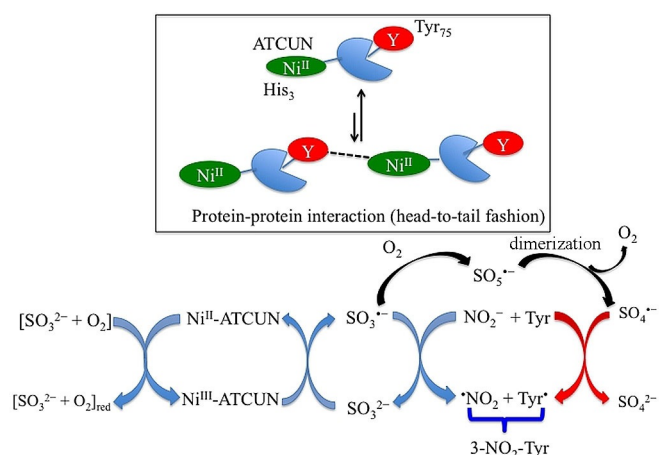


Figure 7. Probable mechanism for the formation of 3-NO₂-Tyr in ATCUN-ORP by using NaNO₂/Na₂SO₃/O₂ and Ni-ATCUN-ORP.

reaction and all of them are reactive species that can likely oxidize redox-active amino acid residues in ATCUN-ORP, such as methionine and tyrosine. The ¹H NMR study (not shown) of the Ni-ATCUN-ORP + (NO₂⁻/SO₃²⁻/O₂) system indicates that the formation of oxysulfur radical cannot oxidize the methionine residue. It is well known that the oxidation of methionine is initiated by HO[•] rather than oxysulfur radicals.^[27,35] Either SO₃^{•-} or SO₄^{•-} radicals or both of them, can be scavenged by nitrite and tyrosine to produce 3-NT. The [•]NO₂ may be obtained from NO₂⁻ in the presence of SO₄^{•-} radicals.^[36] The nitrating species, [•]NO₂ or SO₃^{•-} (or SO₄^{•-}), may abstract phenolic proton from tyrosine residue in ATCUN-ORP to produce Tyr[•] which combined with nitrating species, [•]NO₂ to produce 3-NT. After abstracting proton from tyrosine by oxysulfur radicals, the formation of HSO₃[•] (or HSO₄[•]) can be dissociated to yield HO[•] radical and SO₂²⁻ (or SO₃²⁻)^[34,36] but no detection of HO[•] radical by spin-trap EPR study in the NO₂⁻/SO₃²⁻/O₂ system was observed. So we can rule out the formation of HO[•] radical from this system. The nitrating species is still unknown but it is usually assumed to be nitrogen dioxide due to the transient nature of [•]NO₂. After formation of [•]NO₂ and Tyr[•], their transient nature makes them immediately to react forming non-radical species. It was our initial expectation that [•]NO₂ formed by oxysulfur radicals would react with Tyr[•] to yield 3-NT.

In this study, for the first time, the Ni^{II}-ATCUN in ORP was used as an in vitro model for nitration of tyrosine residues by reacting with the NaNO₂/Na₂SO₃/O₂ system. The UV/Vis absorption and ¹H NMR spectroscopies clearly showed that the ORP-containing ATCUN motif binds Ni^{II} stoichiometrically, to yield a 1:1 Ni^{II}-ATCUN-ORP complex. The Ni^{II}-ATCUN-ORP can be oxidized by either H₂O₂ or SO₃²⁻/O₂ to produce hydroxyl radical as well as oxysulfur radical, respectively. The formation of hydroxyl radicals is not involved in the formation of 3-NT. The former are scavenged by methionine in the vicinity and no more oxidized nitrite is available to yield nitrating species (tyrosine nitration), whereas oxysulfur radical may be scavenged by both nitrite and tyrosine to yield 3-NT. Overall, the accumulated spectroscopic data provide a new pathway formation of nitrating agents for tyrosine nitration, which in vivo may influence

the progression of disease states associated with sulfur metabolism.

Experimental Section

Fusion *D. gigas* protein, ATCUN-ORP, was heterologous expressed in *E. coli* BL21(DE3) and purified in the apo-form as previously described.^[23] Subsequently, 1 mM Ni^{II}Cl₂ was added to 1 mM apo-ATCUN-ORP in 50 mM Tris-HCl, pH 7.5, and the mixture was incubated for 10 min on an ice bath (4 °C) to yield Ni^{II}-ATCUN-ORP derivative. Formation of 3-NT in ATCUN-ORP was assessed by measuring the absorbance at 430 nm at pH 7.6. The reaction was monitored in a 1 cm quartz optical cell, which contained 300 μM Ni^{II}-ATCUN-ORP, 1–5 mM Na₂NO₂ and 0.2–2 mM Na₂SO₃ over 12–15 h under air at room temperature in 50 mM Tris-HCl buffer at pH 7.6. Nitration of tyrosine in ATCUN-ORP was detected by using UV/Vis absorption spectroscopy and monitoring the absorbance at 430 nm.^[31]

Acknowledgements

B.K.M. thanks the Fundação para a Ciência e a Tecnologia, MCTES (FCT/MCTES), for the fellowship grant (SFRH/BPD/63066/2009), which is financed by national funds and co-financed by FSE. L.B.M. thanks FCT/MCTES, for the CEEC-Individual 2017 Program Contract. This work was supported by the Associate Laboratory for Green Chemistry LAQV, which is financed by national funds from Fundação para a Ciência e a Tecnologia, MCTES (FCT/MCTES; UID/QUI/50006/2019). The NMR studies were carried out by using spectrometers of the National NMR Network (RNRMN), also funded by FCT/MCTES (project RECI/BBB-BQB/0230/2012).

Conflict of interest

The authors declare no conflict of interest.

Keywords: ATCUN motif • orange protein • radicals • sulfur metabolism • tyrosine nitration

- [1] a) M. H. Shishebor, R. J. Aviles, M. L. Brennan, X. Fu, M. Goormastic, G. L. Pearce, N. Gokce, J. F. Keaney, Jr., M. S. Penn, D. L. Sprecher, J. A. Vita, S. L. Hazen, *JAMA J. Am. Med. Assoc.* **2003**, *289*, 1675–1680; b) J. F. Reyes, Y. Fu, L. Vana, N. M. Kanaan, L. I. Binder, *Am. J. Pathol.* **2011**, *178*, 2275–2285.
- [2] G. Ferrer-Sueta, N. Campolo, M. Trujillo, S. Bartesaghi, S. Carballal, N. Romero, B. Alvarez, R. Radi, *Chem. Rev.* **2018**, *118*, 1338–1408.
- [3] H. Ischiropoulos, L. Zhu, J. Chen, M. Tsai, J. C. Martin, C. D. Smith, J. S. Beckman, *Arch. Biochem. Biophys.* **1992**, *298*, 431–437.
- [4] N. B. Surmeli, N. K. Litterman, A.-F. Miller, J. T. Groves, *J. Am. Chem. Soc.* **2010**, *132*, 17174–17185.
- [5] B. Bian, Z. H. Gao, N. Weisbrodt, F. Murad, *Proc. Natl. Acad. Sci. USA* **2003**, *100*, 5712–5717.
- [6] D. D. Thomas, M. G. Espey, M. P. Vitek, K. M. Miranda, D. A. Wink, *Proc. Natl. Acad. Sci. USA* **2002**, *99*, 12691–12696.
- [7] L. Qiao, Y. Lu, B. Liu, H. H. Girault, *J. Am. Chem. Soc.* **2011**, *133*, 19823–19831.
- [8] a) B. Sarkar in *Coordination Chemistry*, (Ed. J. P. Laurent), Pergamon Press, Oxford, **1981**, pp. 171–185; b) J. D. Glennon, B. Sarkar, *Biochem. J.* **1982**, *203*, 15–23.
- [9] W. Bal, J. Lukasz, K. S. Kasprzak, *Chem. Res. Toxicol.* **1996**, *9*, 535–540.

- [10] a) P. Neta, R. E. Huie, *Environ. Health Perspect.* **1985**, *64*, 209–217; b) C. Brandt, R. van Eldik, *Chem. Rev.* **1995**, *95*, 119–190.
- [11] S. L. Taylor, N. A. Higley, R. K. Bush, *Adv. Food Res.* **1986**, *30*, 1–76.
- [12] G. C. Brown, R. D. Scholem, H. B. Croll, *Neurology* **1989**, *39*, 252–257.
- [13] L. A. Komarnisky, R. J. Christopherson, T. K. Basu, *Nutrition* **2003**, *19*, 54–61.
- [14] R. Shapiro, *Mutat. Res.* **1977**, *39*, 149–176.
- [15] O. W. Griffith, *Methods Enzymol.* **1987**, *143*, 366.
- [16] H. J. Cohen, I. Fridovich, *J. Biol. Chem.* **1971**, *246*, 359–366.
- [17] J. L. Johnson, W. R. Waud, K. V. Rajagopalan, M. Duran, F. A. Beemer, S. K. Wadman, *Proc. Natl. Acad. Sci. USA* **1980**, *77*, 3715–3719.
- [18] U. Takahama, S. Hirota, *J. Agric. Food Chem.* **2012**, *60*, 1102–1112.
- [19] L. B. Maia, J. J. G. Moura, *Chem. Rev.* **2014**, *114*, 5273–5357.
- [20] B. K. Maiti, R. M. Almeida, L. B. Maia, I. Moura, J. J. G. Moura, *Inorg. Chem.* **2017**, *56*, 8900–8911.
- [21] S. Najmudin, C. Bonifácio, A. G. Duarte, S. R. Pualeta, I. Moura, J. J. G. Moura, M. J. Romão, *Acta Crystallogr. F* **2009**, *65*, 730–732.
- [22] J. P. Laussac, B. Sarker, *Biochemistry* **1984**, *23*, 2832–2838.
- [23] S. R. Pauleta, A. G. Duarte, M. S. Carepo, A. S. Pereira, P. Tavares, I. Moura, J. J. G. Moura, *Biomol. NMR Assignments* **2007**, *1*, 81–83.
- [24] J. E. Subak, Jr., V. M. Loyola, D. W. Margerum, *Inorg. Chem.* **1985**, *24*, 4350–4356.
- [25] a) E. R. Stadtman, *Annu. Rev. Biochem.* **1993**, *62*, 797–821; b) J. Torrealles, M.-C. Guérin, *FEBS Lett.* **1990**, *272*, 58–60.
- [26] a) P. Faller, A. W. Rutherford, R. J. Debus, *Biochemistry* **2002**, *41*, 12914–12920; b) J. J. Warren, J. R. Winkler, H. B. Gray, *FEBS Lett.* **2012**, *586*, 596–602.
- [27] a) C. Jacob, G. Giles, N. M. Giles, H. Sies, *Angew. Chem. Int. Ed.* **2003**, *42*, 4742–4758; *Angew. Chem.* **2003**, *115*, 4890–4907; b) I. Spasojević, P. J. Bogdanović, L. Vujisić, M. Spasić, *Amino Acids* **2012**, *42*, 2439–2445.
- [28] Y.-Y. Fang, C. A. Claussen, K. B. Lipkowitz, E. C. Long, *J. Am. Chem. Soc.* **2006**, *128*, 3198–3207.
- [29] V. Lepentsiotis, J. Domagala, I. Grgic, R. V. Eldik, J. G. Muller, C. J. Burrows, *Inorg. Chem.* **1999**, *38*, 3500–3505.
- [30] O. Augusto, M. G. Bonini, A. M. Amanso, E. Linares, C. C. Santos, S. L. De Menezes, *Free Radical Biol. Med.* **2002**, *32*, 841–859.
- [31] a) V. De Filippis, R. Frasson, A. Fontana, *Protein Sci.* **2006**, *15*, 976–986; b) J. F. Riordan, M. Sokolovsky, B. L. Vallee, *Biochemistry* **1967**, *6*, 358–361.
- [32] B. K. Maiti, L. B. Maia, S. R. Pauleta, I. Moura, J. J. G. Moura, *Inorg. Chem.* **2017**, *56*, 2210–2220.
- [33] H. Zhang, J. Joseph, C. Felix, B. Kalyanaraman, *J. Biol. Chem.* **2000**, *275*, 14038–14045.
- [34] M. Velayutham, C. F. Hemann, A. J. Cardounel, J. L. Zweier, *Biochem. Biophys. Rep.* **2016**, *5*, 96–104.
- [35] S. F. Yang, *Biochemistry* **1970**, *9*, 5008–5014.
- [36] Y. Ji, L. Wang, M. Jiang, J. Lu, C. Ferronato, J. M. Chovelon, *Water Res.* **2017**, *123*, 249–257.

Manuscript received: December 14, 2018

Accepted manuscript online: February 4, 2019

Version of record online: March 4, 2019
